Application of Co/Al$_2$O$_3$ catalyst in steam reforming of glycerol

Chin Kui Cheng, Say Yei Foo, Adesoji A. Adesina*

Reactor Engineering & Technology Group,
School of Chemical Engineering, The University of New South Wales, Sydney,
New South Wales, Australia 2052
*Email: a.adesina@unsw.edu.au

ABSTRACT

Alumina-supported cobalt catalyst has been employed in a fixed bed reactor for the direct production of synthesis gas from glycerol steam reforming. Physicochemical properties of the Co/Al$_2$O$_3$ catalyst were determined from N$_2$ physisorption, H$_2$ chemisorption, CO$_2$ and NH$_3$-TPD study as well as X-ray diffraction analysis. Both Lewis and Brönsted acid sites are present on the catalyst surface. The acid:basic site ratio is about 6. Glycerol conversion of between 30 to 65% with relatively large H$_2$:CO ratio (6 to 12) and near-stoichiometric values of H$_2$:CO$_2$ ratio (2 to 2.20) were obtained depending on feed composition (30 to 60wt% glycerol mixture). The glycerol consumption rate appeared to be a weak function of glycerol (0.1) and has 0.4 order with respect to the steam partial pressure. Increased glycerol partial pressure led to high carbon deposition (TOC values of 20 to 24%). However, removal of the deposited carbon was essentially complete following a TPO(air)-TPR(H$_2$) scheme.

INTRODUCTION

The demand for hydrogen has increased substantially in recent years due to the global energy consumption as well as significant developments in fuel cell technologies. The indiscriminate use of fossil fuels has contributed to the excessive emission of CO$_2$ into the atmosphere with associated detrimental effects on global weather pattern. In order to mitigate this problem, H$_2$ has received attention as an important alternative fuel. One of the techniques to produce H$_2$ is through steam reforming of renewable resources such as carbohydrate.

Glycerol is a non-edible byproduct formed during the biodiesel synthesis. In particular, the conversion of waste glycerol to high value-added product is desirable. Recent efforts on the aqueous phase reforming of various carbohydrates by Dumesic and co-workers have demonstrated the promise of H$_2$ or syngas production from biowastes (Dumesic et al., 2004, 2005). The present work examines the steam reforming of glycerol, thus, the pertinent reactions are:

$$C_3H_8O_3 \text{ (g)} + 3H_2O \text{ (g)} \leftrightarrow 3CO_2 \text{ (g)} + 7H_2 \text{ (g)} \tag{1}$$
$$C_3H_8O_3 \text{ (g)} \leftrightarrow 3CO \text{ (g)} + 4H_2 \text{ (g)} \tag{2}$$
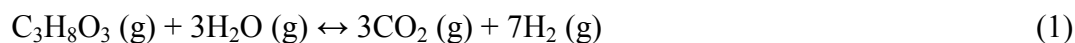
Both reactions are strongly endothermic and thus carried out at temperatures greater than 500 K. The quantities of CO, CO$_2$ and H$_2$ produced depend on reaction conditions such as steam to glycerol ratio, temperature and also the pressure of reaction. Supported transition metals in Group VII such as Pt, Pd, Ru, Rh, Co and Ni were shown to have good activity for glycerol steam reforming (Hirai et al., 2005; Buffoni et al., 2009; Profetti et al., 2009; Iriondo et al., 2008, 2009; Adhikari et al., 2007, 2008). Significantly, Simonetti and co-workers (2007) showed that CO turnover frequency was

fractional order with respect to glycerol (0.1–0.2) with activation barriers of 60–90 kJ mol^{-1} over carbon-supported Pt and Pt-Rh catalysts while Adhikari et al. (2009) reported activation energy of 103.4 kJ mol^{-1} and reaction order of 0.233 over Ni/CeO$_2$ catalyst. The current work was undertaken to examine the kinetic behaviour of glycerol reforming over monometallic Co/Al$_2$O$_3$ catalyst.

EXPERIMENTAL

Catalyst Preparation and Characterization

15wt% Co/Al$_2$O$_3$ catalyst was prepared using wetness impregnation technique. The preparation method is detailed elsewhere (Cheng & Adesina, 2010). The BET surface area and pore-size distribution of the calcined samples were determined from N$_2$ physisorption at 77 K in a Quantachrome Autosorb unit. Prior to the analysis, the fresh catalysts were pretreated under vacuum condition at 573 K for at least 3 h. Powder X-ray diffraction (XRD) patterns of the calcined catalysts were obtained on X'pert Pro Multi-purpose X-ray Diffraction (MPD) system using Cu K$_\alpha$ radiation (λ = 0.154 nm) operated at 40 mA and 45 kV. The diffractograms were analysed using X'Pert ScorePlus software. Crystallite sizes were calculated using Scherrer equation, $d = 0.94\lambda/(\beta\cos\theta)$, where d is the crystallite size, λ is the wavelength of the radiation, β is the full-width at half maximum (FWHM) of the diffraction peak and θ is the half of the diffraction angle. Metal dispersion was evaluated from H$_2$ chemisorption runs performed on Micromeritics 2910 unit (Micromeritics Instrument Corp.). The acidic and basic properties of the catalysts were evaluated using temperature-programmed desorption (TPD) employing NH$_3$ and CO$_2$ as reactant gases respectively. Thermogravimetric analysis of the calcination and reduction characteristics of fresh catalysts was performed using a ThermoCahn TG 2121 system. Temperature-programmed calcination was carried out at 873 K, for 5 h, with heating rates of 5, 10 and 20 K min^{-1} using 55 ml min^{-1} high purity air. Temperature programmed reduction (TPR) was performed up to 973 K, for 5 h, at 5 K min^{-1}, in 55 ml min^{-1} of 50% H$_2$/N$_2$ mixture for the fresh oxide catalysts. The measurements were obtained in terms of catalyst weight loss due to thermal treatment. The results were used to determine the appropriate calcination and reduction temperatures for Co/Al$_2$O$_3$ catalyst. In addition, the solid state kinetic analysis was also performed on the TGA data.

Experimental Apparatus and Kinetic Studies

Glycerol steam reforming reaction experiments were conducted in a stainless-steel fixed bed micro-reactor sizing 10 mm *i.d.* Kinetic data were collected at atmospheric pressure and reaction temperature between 723 K to 823 K. Glycerol-water mixture with composition 30wt% to 60wt% was used as feed to ensure excess steam. For differential reactor operation, and minimize various transport-induced pathological conditions, the ratio of catalyst bed length to particle diameter (L/D$_p$) was 80, and the ratio of inner diameter of reactor to particle diameter (D/D$_p$) was 71.5. These values were within acceptable values recommended by Froment and Bischoff (1990). Catalyst particle size between 90 to 140 μm and gas hourly-space velocity of 5.0×10^4 mL g$_{cat}^{-1}$ hr^{-1} were employed to minimize internal pore and external transport limitations.

The performance was evaluated in terms of conversion into gaseous product (based on a carbon balance between the inlet and the outlet of the reactor), selectivity and also yield which were defined as

$$\text{Conversion to gaseous product, } X_G(\%) = \frac{F_{dry,out}\sum y_{C,out}}{F_{C,in}} \times 100 \qquad (3)$$

$$\text{Selectivity of product } i, \ S_i(\%) = \frac{r_i}{\sum r_i} \times 100 \qquad (4)$$

$$\text{Yield of product } i, \ Y_i = \frac{r_i}{\left(-r_{C_3H_8O_3}\right)} \qquad (5)$$

where F and y_C are relevant molar flow rates (mol s^{-1}) and gas mol fractions respectively, the subscript 'C,out' indicating all detected carbon-containing gas products and $F_{dry,out}$ is the dry total molar flow of gases leaving the reactor, r_i = formation rate of gaseous products, the summation term $\left(\sum r_i\right)$ has considered H_2, CO_2, CO and CH_4 formation rates while $\left(-r_{C_3H_8O_3}\right)$ is the glycerol consumption rate.

Characterization of Carbon Deposition

Used catalysts from the reforming runs were subjected to carbon analysis. The total organic carbon (TOC) analysis was performed in Shimadzu TOC Analyzer SM-5000A. Typically, about 10 mg of used catalyst was used in each measurement. In addition, the used catalysts were subjected to temperature-programmed evaluation *viz.* TPR-TPO and TPO-TPR schemes. All the carbon gasification studies were carried out in ThermoCahn TG 2121 unit. For each step, ramping rate of 10 K min^{-1} from room to final temperature of 973 K was employed, followed by holding time of 1 h at 973 K. In the TPR step, 50% mixture of H_2/Ar was used while purified air was chosen for the TPO step. In a typical run, total outlet gas flow rate was 120 mL min^{-1}. All the gases were dehumidified prior to use. Used catalyst samples were dried *in-situ* under an Ar blanket at 403 K for 1 h prior to on-line weight analysis.

RESULTS AND DISCUSSION

Catalyst Characterisation

Table 1 shows that calcination at 873 K caused a mild reduction in BET area and pore volume of the alumina support with further reduction (21.5%) in these properties upon metal impregnation probably due to metal particle blockage of the support pore structure. H_2 chemisorption data revealed that metal particle size was 66.5 nm although Scherrer equation based on the XRD data (Fig. 1) gave 51.5 nm. This value approximates the metal particle size calculated from H_2 chemisorption analysis.

Tab. 1: Physicochemical properties of Al_2O_3 and fresh Co/Al_2O_3 catalysts.

Properties	Fresh Al_2O_3	Calcined Al_2O_3	Co/Al_2O_3
BET surface area (m^2 g^{-1})	228.6	210.6	165.4
Pore volume (ml g^{-1})	0.7066	0.6876	0.554
Pore diameter (Å)	123.7	130.6	121.9

Dispersion (%)		-	-	1.50
Metal surface area (m^2 g^{-1})		-	-	1.521
Metal particle diameter (nm)		-	-	66.48
Crystallite size (nm)		-	-	51.51
NH_3 desorption heat,	Peak I	-	68.90	50.53
ΔH_{NH_3} (kJ mol^{-1})	Peak II	-	-	96.29
CO_2 desorption heat,	Peak I	-	63.20	54.19
ΔH_{CO_2} (kJ mol^{-1})	Peak II	-	68.40	33.18
Acid site conc.	Peak I	-	2.13	0.93
(μmol m^{-2})	Peak II		N/A	1.95
Basic site conc.	Peak I	-	0.14	0.25
(μmol m^{-2})	Peak II		0.32	0.27
Acid:Basic site ratio	Peak I	-	15.40	3.70
	Peak II		N/A	7.20
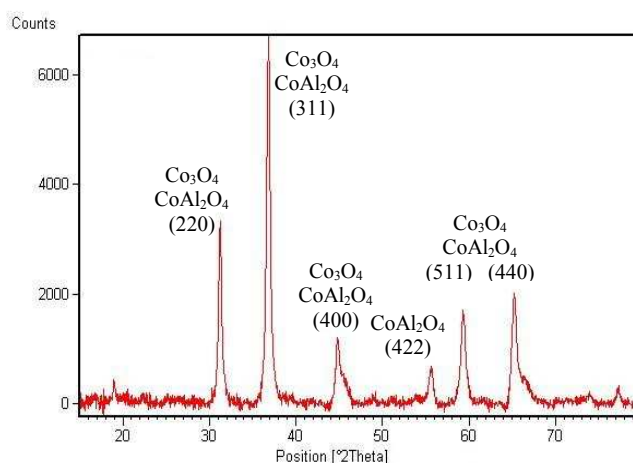
Fig. 1: XRD patterns of the Co/Al_2O_3.

The acid/basic nature of catalyst sites on Co/Al_2O_3 was studied using TPD method. CO_2-TPD showed two distinct peaks indicating two different basic sites. Formal treatment of the data at different heating rates gave 54.19 kJ mol^{-1} and 33.18 kJ mol^{-1} for peak I (373 K to 413 K) and II (688 K to 798 K) respectively. Peak I is indicative of the presence of Lewis sites while Peak II was associated with Brönsted sites. The presence of two distinct peaks was also observed for NH_3-TPD analysis, *viz.*; a weak Lewis acid centre in the low temperature peak region (533 K to 578 K), and a high temperature peak (663 K to 708 K) indicative of a Brönsted acid site. The heat of NH_3 desorption was 50.53 kJ mol^{-1} for Lewis site and 96.29 kJ mol^{-1} for the Brönsted acid site. Similar analysis performed on calcined alumina support revealed the presence of Lewis acid site only with magnitude of 68.90 kJ mol^{-1}. However, both Lewis and Brönsted basic sites were present on calcined alumina support (cf. Table 1). Significantly, this indicates that Bronsted acid site was located at the interface of metal-alumina support while basic site for Co/Al_2O_3 catalyst is in fact most likely located on alumina support judging from almost similar basic sites concentration (0.25 and 0.27 μmol m^{-2} for Co/Al_2O_3 catalyst as opposed to 0.14 and 0.32 μmol m^{-2} for calcined alumina support only).

The formation of different oxide phases in the catalyst after calcination and its subsequent reducibility is a determinant of catalyst performance. The TGA profile for calcination shows that the metal nitrate decomposition to oxides took place below 723 K regardless of the heating rate. There was no weight loss beyond 773 K. However, higher heating rate appears linked to higher calcination rate. A single sharp peak was observed at around 448 K corresponds to the formation of Co_3O_4. This is shown as

$$Co(NO_3)_2 \rightarrow CoO + N_2O_5 \tag{6}$$
$$CoO + Al_2O_3 \rightarrow CoAl_2O_4 \tag{7}$$
$$3CoO + \tfrac{1}{2}O_2 \rightarrow Co_3O_4 \tag{8}$$

In addition, a small shoulder peak was formed at around 523 K representing the formation of $CoAl_2O_4$ phase. The absence of a separate CoO phase from XRD analysis indicates the complete consumption of all the initial Co(II) oxide formed from Eqn. (6) in Eqns. (7) and (8). Beyond these decomposition temperatures, the oxide catalysts remained practically stable up to 873 K. The formation of oxide species from TGA analysis was consistent with the XRD results shown in Fig. 1. The formation of Co_3O_4 and $CoAl_2O_4$ was recognised through strong peak intensities shown at $2\theta = 31^o$ and 37° respectively.

The H_2 TPR spectrum showed the reduction of Co_3O_4 phase for 15wt% Co/Al_2O_3 catalyst (figure not shown). Three hydrogen consumption peaks showed the reduction of Co_3O_4 to CoO (at 753 K) followed by further reduction of CoO to Co species (shoulder peak at 793 K) while another smaller shoulder peak at 853 K represents the reduction of metal aluminate species to a more stable metal-Al_2O_3 phase.

$$Co_3O_4 + H_2 \rightarrow 3CoO + H_2O \tag{9}$$
$$CoO + H_2 \rightarrow Co + H_2O \tag{10}$$
$$Co\text{-}Al_2O_4 + H_2 \rightarrow Co + Al_2O_3 + H_2O \tag{11}$$
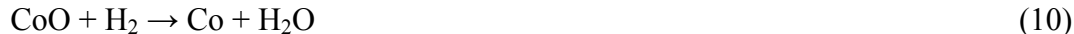
Reaction Studies

Catalytic Activities

The steam reforming of glycerol was studied using different aqueous glycerol solutions, 30- 60wt% corresponding to a steam-to-carbon ratio (SCR) of 1.1 to 4.0. It was found that at 823 K, conversion to gaseous products was highest for 30% glycerol (75%) and lowest for 60% glycerol (25.0%). Conversions recorded at 40wt% and 50wt% were 52% and 34% respectively. It seems that the increase in glycerol conversion with higher steam partial pressure was mainly attributed to the enhancement of CO_2 production from Eqn. (1).

The transient kinetic behaviour was identical over the whole range of aqueous glycerol mixture used in this experiment. As such, only the transient catalytic performance evaluated from the activity tests for 40 wt% glycerol steam reforming at 823 K is presented in Fig. 2. Blank tests using the same feed and either an empty or calcined Al_2O_3 support yielded negligible glycerol conversion. Fig. 2 shows the transient composition profile of H_2, CO_2, CO and CH_4. It is apparent that steady-state was attained for H_2 and CO_2 after about one hour on-stream. Significantly, it shows that approximately 23 mol% of H_2 were produced. In addition, a relatively stable production of CO_2 at 10 mol% was achieved. As such, the ratio between H_2 and CO_2 is approximately 2.3. A complete single reaction between glycerol and steam in theory

produces 3 mols of CO_2 and 7 mols of H_2, translating into stoichiometry value of 2.33. Hence, stoichiometry value was nearly achievable over Co/Al_2O_3 catalyst. The yield of CO and CH_4 however gradually decreased over the entire reaction period. The similar transient characteristic for CO and CH_4, which was nevertheless different from H_2 and CO_2 seems to indicate that the reaction pathways were not same for both sets of products. In fact, both were produced at the onset of reaction, which suggests that methanation reaction played minimal role during steam reforming of oxygenated hydrocarbons. The ratio of $CO_2:CO > 1$ as depicted by Fig. 2 is consistent with the presence of C−O and O−H bonds in glycerol molecule itself, hence it is more likely to be steam-reformed into CO_2 as shown by Eqn. (1).
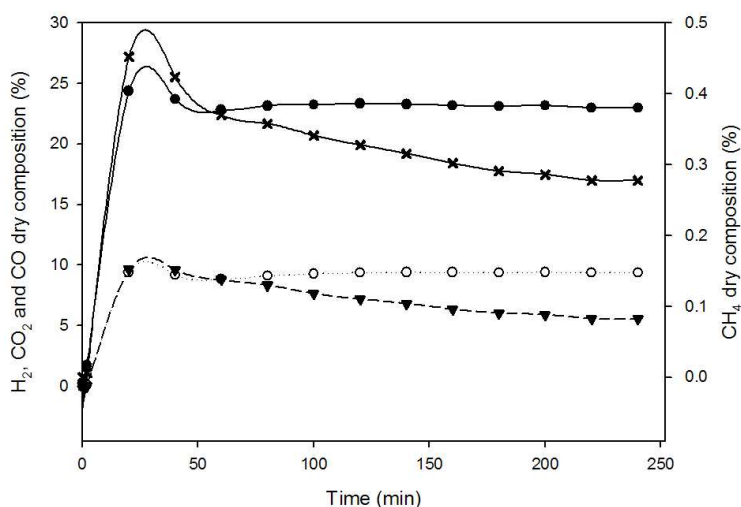
Fig. 2: The transient dry composition profiles of H_2 (●), CO_2 (○), CO (▼) and CH_4 (x) in glycerol steam reforming. Conditions: 823 K; $P_{glycerol} = 7.40$ kPa, $P_{steam} = 57.0$ kPa; WHSV $= 5.0 \times 10^4$ mL g_{cat}^{-1} hr^{-1}.

The drop in CO and CH_4 compositions was probably because both CO and CH_4 formed as intermediate species that covered the catalyst surface (deactivation process) via Boudouard reaction and methane decomposition. This is consistent with generally accepted argument that deposition of carbon onto clean catalyst surface is very rapid at the initial stage of reaction, thereafter it gradually levelling-off (Bartholomew et al., 1988). This trend was reasonably captured by CO and CH_4 transient profile (cf. Fig. 2). Nonetheless, the deactivation of Co/Al_2O_3 catalyst was mild as shown by almost constant production of H_2 and CO_2.

In order to gain understanding of reaction scheme for glycerol steam reforming, the selectivity and yield variation with partial pressure of both reactants ($P_{glycerol}$ and P_{steam} at 823 K) as well as temperature variation were plotted and shown in Figs. 3 to 5. Under excess steam condition, H_2, CO_2 and CO always constituted the majority of gaseous products. This indicates that Eqns. (1) and (2) were indeed the primary reactions. As shown by Figs. 3 and 4, the product selectivity and yield were essentially invariant with increasing $P_{glycerol}$ suggesting that the same reaction steps were dominant for both low and high $P_{glycerol}$. Importantly, it suggests that chemisorption of glycerol was weak on catalyst surface which ultimately contributed to the insensitivity of C_1 species with $P_{glycerol}$. However, effect of steam partial pressure revealed a rapid drop in

the selectivity and yield of CO with increasing P_{steam} which was most likely due to WGS reaction. Coincidentally, within the same P_{steam} window, selectivity and yield of CO_2 and H_2 increased slightly or nearly unchanged. This is because CO present in much smaller quantity compared to H_2 and CO_2 at 823 K. In addition, the accompanying slight improvement in CH_4 yield with P_{steam} seems to indicate that part of the CH_4 was directly generated from the reaction between glycerol and H_2 in a hydrogenolysis reaction.

(a)   (b)
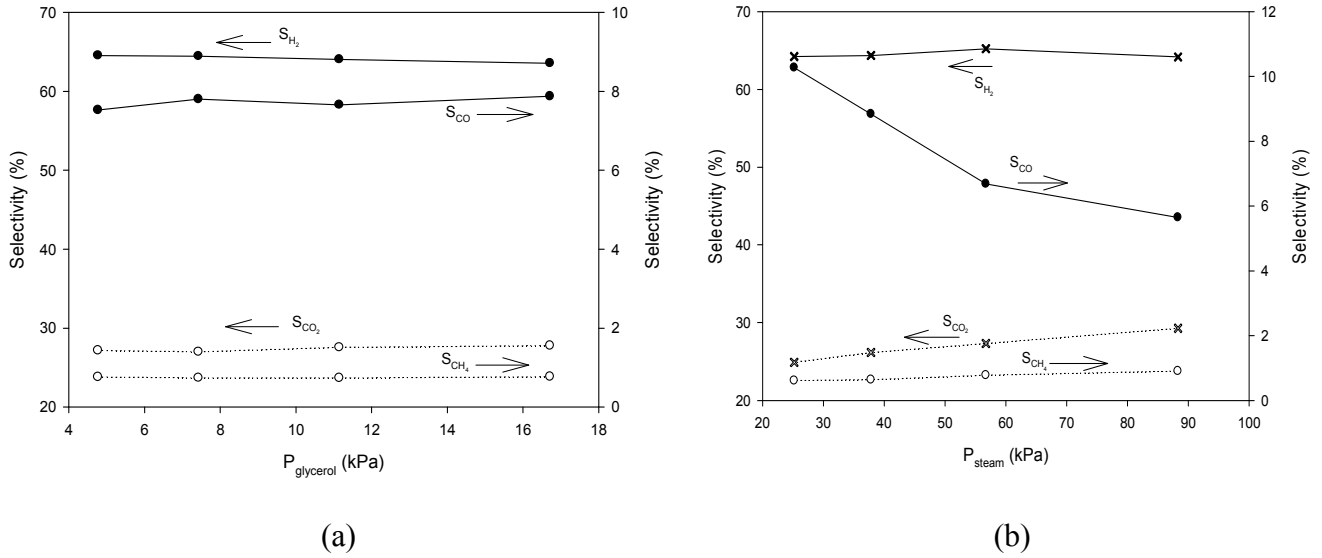
Fig. 3: Selectivity of product as function of $P_{glycerol}$ and P_{steam} at temperature of 823 K.

(a)   (b)
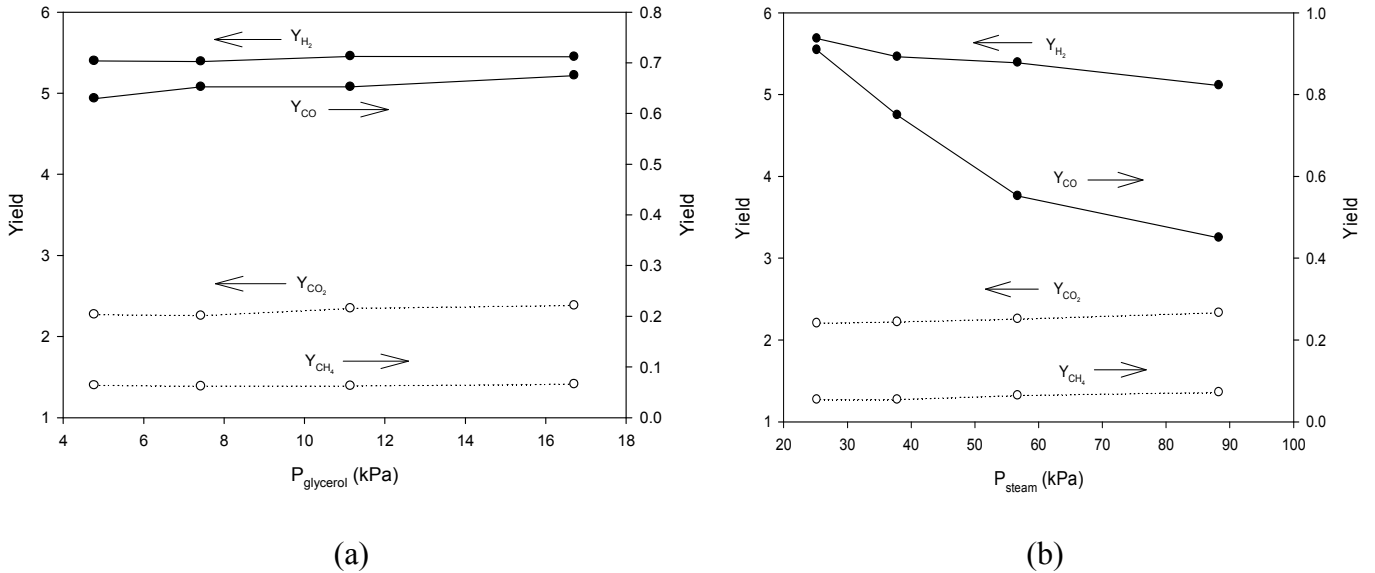
Fig. 4: Yield of product as function of $P_{glycerol}$ and P_{steam} at temperature of 823 K.

The effect of temperature on product distribution is illustrated in Fig. 5. Significantly, H_2 and CO_2 showed improvement with increasing temperature, consistent with endothermic nature of Eqn. (1). Within the same temperature range, CO selectivity dropped with increased temperature as may be expected from the exothermic character of WGS reaction. In addition, the increase in CH_4 amount with reaction temperature seems to indicate that gasification of carbonaceous species on Co/Al_2O_3 catalyst became

more dominant at higher reaction temperatures. However, the quantity of CH_4 produced was small and did not affect the overall yield of H_2.

(a)   (b)
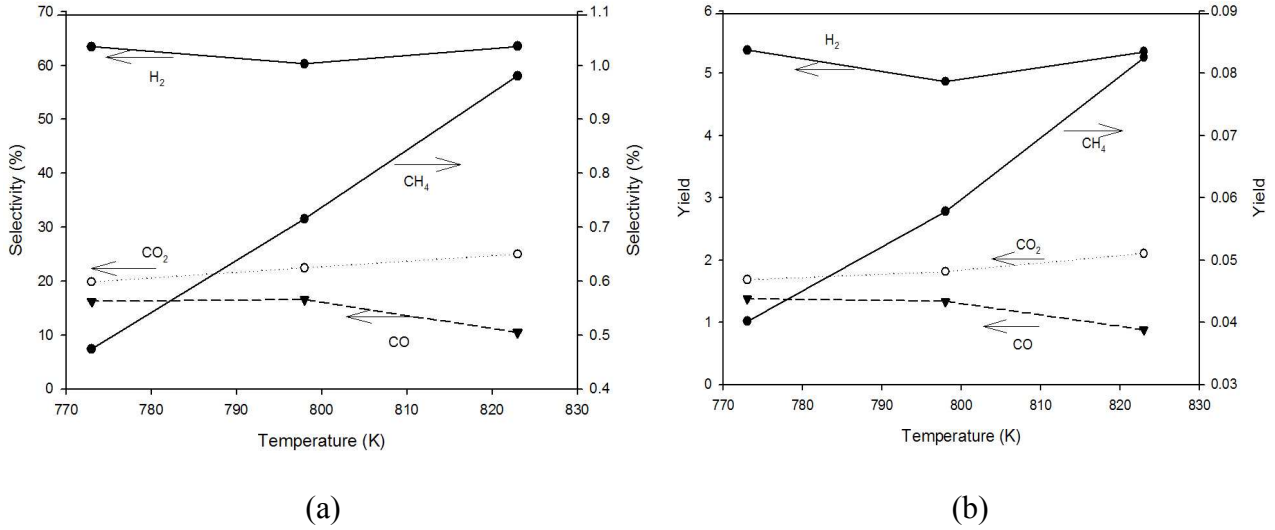
Fig. 5: Selectivity and yield of product as function of temperature at $P_{glycerol}$ = 7.40 kPa, P_{steam} = 57.02 kPa; WHSV = 5.0 ×10^4 mL g_{cat}^{-1} hr^{-1}.

Power Law and Arrhenius-Behaviour Modelling

Glycerol reforming rate and formation rates of H_2, CO_2, CO and CH_4 were fitted to a power-law model

$$(r_i) = kP_{glycerol}^{\alpha}P_{steam}^{\beta} \qquad\qquad i = H_2, CO_2, CO \text{ or } CH_4 \qquad (12)$$

where k is the reforming rate constant, $P_{glycerol}$ and P_{steam} are reactants' partial pressure while α and β are the corresponding orders of reaction. Regression of the rate data gave the parameter estimates provided in Table 2.

Tab. 2: Estimates of parameters for glycerol steam reforming (nonlinear least squares).

Major product	$k (10^6)$ at 823 K mol m^{-2} s^{-1} kPa$^{-(\alpha+\beta)}$	α	β
$C_3H_8O_3$	1.987	0.08	0.39
H_2	13.660	0.10	0.32
CO_2	3.061	0.13	0.44
CO	32.230	0.16	-0.18
CH_4	0.055	0.10	0.66

All species showed positive α-values which is an indication of direct generation of H_2, CO_2, CO and CH_4 from glycerol during the reaction. Furthermore, the small α-values for the C_1 products implicate weak adsorption of glycerol species on catalyst surface. This is also seen in the near constant selectivity and yield of CO_2, CO and CH_4 products on $P_{glycerol}$ as shown in both Figs. 3(a) and 4(a). The steam inhibition (negative β value) of CO rate is an indication of either competitive adsorption of steam on the same site as CO (especially at the relatively high steam partial pressure used) or the loss of CO produced via WGS reaction to CO_2 and H_2 as indicated by product yield and selectivity as function of P_{steam} in Figs. 3(b) and 4(b). Furthermore, by employing the Arrhenius equation $k = Ae^{-E_A/RT}$ at different reaction temperatures (723 K, 773 K and 823 K), the

activation energy E_A and pre-exponential factor, A were calculated. A linear regression of the experimental data points gave $R^2 > 0.99$ (figure not shown). Table 3 shows the summary of E_A and A values. H_2 and CO_2 which constitute the major reforming products have E_A of 66.8 and 78.3 kJ mol^{-1} respectively. In addition, the E_A of 102.0 kJ mol^{-1} for CH_4 species shows that it is not a primary product of the reaction but possibly produced via secondary reactions.

Tab. 3: Kinetic parameters calculated from the rate equation based on the power-law.

Pre-exponential factor A (mmol m^{-2} s^{-1})					E_A (kJ mol^{-1})				
$C_3H_8O_3$	H_2	CO_2	CO	CH_4	$C_3H_8O_3$	H_2	CO_2	CO	CH_4
36.52	235.6	282.9	3.00	184.3	67.20	66.76	78.25	31.09	102.84

Characterization of Used Catalysts

Carbon deposition was evident on the used catalyst samples. Fig 6 shows the total organic carbon (TOC) deposited on catalysts as function of partial pressures of both glycerol and steam at 823 K after 4 h of experimental run. In general, carbon deposition occurs even under stoichiometrically excess steam-to-glycerol ratios (30wt% to 60wt% glycerol). The carbon deposition is strongly dependent on the partial pressure of glycerol. In contrast, it is weakly inhibited by the presence of steam. To examine the characteristic of deposited carbon, TPO-TPR and TPR-TPO schemes were employed. TPO-TPR cycles (cf. Fig. 7a) show a complete burn-off of carbon deposited on used catalyst. This is evidenced by the dramatic drop in the weight of the catalyst sample. In the subsequent step (TPR), reduction of metal oxides occurred and this reduced the weight of sample. The second scheme (cf. Figure 7b), TPR-TPO cycles show poor gasification of the carbon deposited in the first step when hydrogen was used as reactant gas (TPR). It requires the second step which employed air as reactant gas to achieve complete burn-off of carbon. The different reactivity of carbon deposited on the surface of coked catalyst is an indication of the presence of at least two types of carbon pools on the catalyst surface, for which, one type is reactive towards H_2 (C_α) while another pool of carbon seems to be inert towards H_2 and only reactive towards O_2 (C_β).
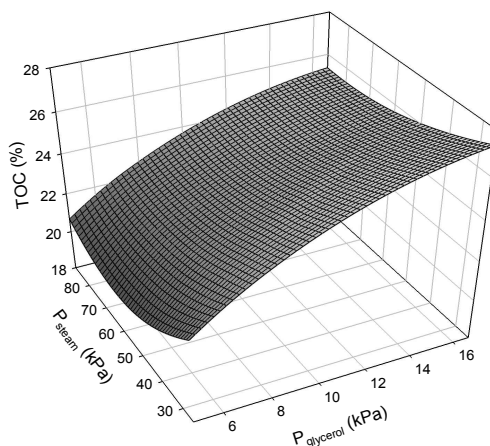
Fig. 6: Amount of organic carbon deposited on Co/Al$_2$O$_3$ catalyst at 823 K.

9

(a)   (b)
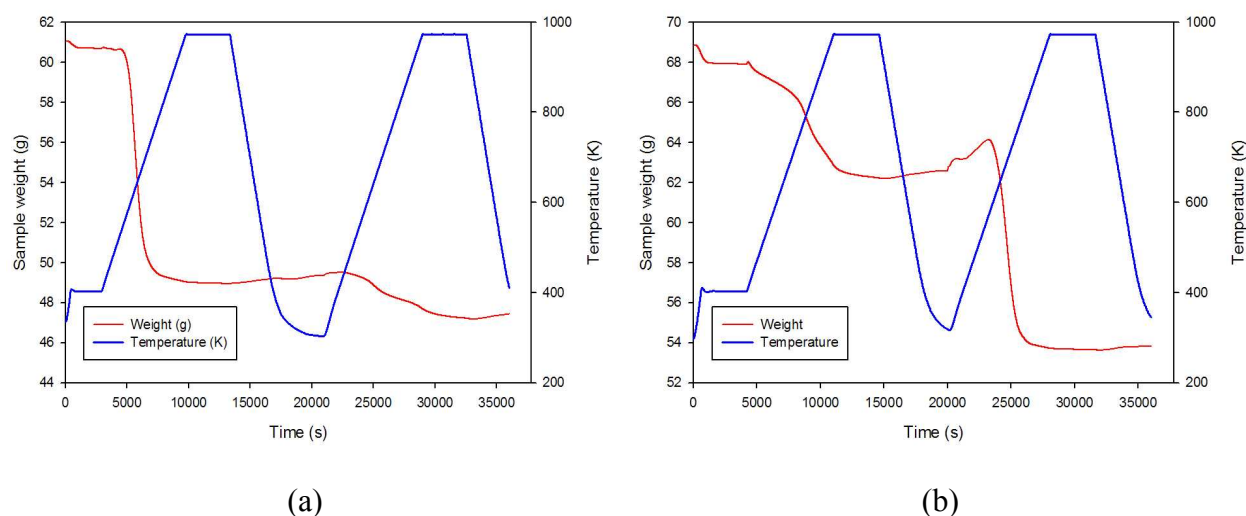
Fig. 7: Gasification of deposited carbon employing (a) TPO-TPR scheme and (b) TPR-TPO scheme.

CONCLUSIONS

Alumina-supported cobalt catalyst was prepared for glycerol steam reforming. CO_2 and NH_3-TPD study showed that the catalyst surface was mainly populated by Lewis and Brönsted acid sites with acid:basic site ratio of about 6. Glycerol conversion of between 30 to 65% with relatively large H_2:CO ratio (6 to 12) and near-stoichiometric values of H_2:CO_2 ratio (2 to 2.20) were obtained depending on feed composition (30 to 60wt% glycerol mixture). Small amount of CH_4 were also being co-produced. The glycerol consumption rate appeared to be a weak function of glycerol (0.1) and has 0.4 order with respect to the steam partial pressure. Increased glycerol partial pressure led to high carbon deposition (TOC values of 20 to 24%). However, removal of the deposited carbon was essentially complete following a TPO(air)-TPR(H_2) scheme.

REFERENCES

Adhikari, S, Fernando, S & Haryanto, A 2007, 'Production of hydrogen by steam reforming of glycerin over alumina-supported metal catalysts', *Catalysis Today*, vol. 129, p. 355.

Adhikari, S, Fernando, SD & Haryanto, A 2008, 'Hydrogen production from glycerin by steam reforming over nickel catalysts', *Renewable Energy*, vol. 33, p. 1097.

Adhikari, S, Fernando, SD & Haryanto, A 2009, 'Kinetics and reactor modeling of hydrogen production from glycerol via steam reforming process over Ni/CeO$_2$ catalysts', *Chemical Engineering Technology*, vol. 32, p. 541

Buffoni, IN, Pompeo, F, Santori, GF & Nichio, NN 2009, 'Nickel catalysts applied in steam reforming of glycerol for hydrogen production', *Catalysis Communications*, vol. 10, p. 1656.

Bartholomew, CH, Strasburg, MV & Hsieh, HY 1988, 'Effects of support on carbon formation and gasification on nickel during carbon monoxide hydrogenation', Applied Catalysis, vol. 36, p.147.

Cheng, CK & Adesina, AA, 'Glycerol steam reforming over bimetallic Co-Ni/Al$_2$O$_3$', *Ind. Eng. Chem. Res.* (in press)

Davda, RR, Shabaker, JW, Huber, GW, Cortright, RD & Dumesic, JA 2005, 'A review of catalytic issues and process conditions for renewable hydrogen and alkanes by aqueous-phase reforming of oxygenated hydrocarbons over supported metal catalysts', *Applied Catalysis B: Environmental*, vol. 56, p. 171.

Froment, GF & Bischoff, KB 1990, 'Chemical reactor analysis and design', John Wiley & Sons, New York.

Hirai, T, Ikenaga, N-O, Miyake, T & Suzuki, T 2005, 'Production of hydrogen by steam reforming of glycerin on ruthenium catalyst', *Energy and Fuels*, vol. 19, p. 1761.

Iriondo, A, Barrio, VL, Cambra, JF, Arias, PL, Guemez, MB, Navarro, RM, Sanchez-Sanchez, MC & Fierro, JLG 2008, 'Hydrogen production from glycerol over nickel catalysts supported on Al_2O_3 modified by Mg, Zr, Ce or La', *Topics in Catalysis*, vol. 49, p. 46.

Iriondo, A, Barrio, VL, Cambra, JF, Arias, PL, Güemez, MB, Navarro, RM, Sanchez-Sanchez, MC & Fierro, JLG 2009, 'Influence of La_2O_3 modified support and Ni and Pt active phases on glycerol steam reforming to produce hydrogen', *Catalysis Communications*, vol. 10, p. 1275.

Profeti, LPR, Ticianelli, EA & Assaf, EM 2009, 'Production of hydrogen via steam reforming of biofuels on Ni/CeO_2-Al_2O_3 catalysts promoted by noble metals', *International Journal of Hydrogen Energy*, vol. 34, p. 5049.

Shabaker, JW, Huber, GW & Dumesic, JA 2004, 'Aqueous-phase reforming of oxygenated hydrocarbons over Sn-modified Ni catalysts', *Journal of Catalysis*, vol. 222, p. 180.

Simonetti, DA, Kunkes, EL & Dumesic, JA 2007, 'Gas-phase conversion of glycerol to synthesis gas over carbon-supported platinum and platinum-rhenium catalysts', *Journal of Catalysis*, vol. 247, p. 298.

BRIEF BIOGRAPHY OF PRESENTER

Chin Kui Cheng

Chin Kui Cheng is currently a PhD student at UNSW. His doctoral thesis deals with the steam reforming of glycerol. He is on study leave from Universiti Malaysia Pahang, Kuantan, Malaysia.